

# An Engineering Study of the Colloid-Fueled Reactor Concept

Y. S. TANG,\* J. S. STEFANKO,† P. W. DICKSON,‡ AND D. W. DRAWBAUGH§  
Westinghouse Electric Corporation, Pittsburgh, Pa.

**A concept using colloid fuel, vortex chamber cavity is described. The reactor uses particulate fuel with a composition (1U-10Zr)C where uranium is U-233. The fuel is fed to the cavity by hydrogen gas. The cavity, a compressed vortex chamber has an  $L/D$  ratio of 0.15 in the fuel region. Beryllium is used as the reflector material and is contained in a titanium-alloy (Ti-Al-V) pressure vessel. The reactor is designed for ground test purpose and would generate a 45,000 kg (100,000 lb) thrust with a specific impulse of 1200 sec. The over-all dimensions of the pressure vessel are approximately 240 cm (95 in.) diam and 240 cm (95 in.) in length. The engine weighs 19,000 kg (41,000 lb).**

## Introduction

THE nuclear rocket engine promises to out-perform the best conceivable chemical propulsion system by a wide margin. The solid-core reactor concept, representing the state-of-the-art in nuclear propulsion systems, offers a specific impulse ( $I_{sp}$ ) greater than chemical propulsion system by more than a factor of two.<sup>1</sup> The gaseous-core concept, representing an advanced system, can theoretically provide a value of  $I_{sp}$  on the order of five to nine times that of chemical systems.<sup>2,3</sup> Both the fuel loss rate and the engine weight have been the major considerations for the feasibility of the gaseous-core concept. The concept of a colloid-fueled reactor on the other hand may be considered as an intermediate step between the solid-core and gaseous-core reactors.<sup>4</sup>

A colloid-fueled nuclear rocket engine utilizes fuels in the colloidal form, i.e., solid particles or liquid droplets with the gaseous propellant. The suspension of the fuel is caused by the centrifugal force generated in the cavity. Intimate contact, and consequently good heat transfer, between the fuel and propellant are maintained. This results in higher temperatures than those obtainable in solid-core reactors. However since significant vaporization would result in fuel losses, the propellant temperature is limited to a level lower than that of a gaseous-core reactor. The concept has been first evaluated by the Aerospace Research Laboratory (ARL) of Wright-Patterson Air Force Base. ARL developed a highly effective vortex chamber configuration which has an excellent separation capability.<sup>5</sup> In conjunction with this development, an engineering study of the concept was also carried out. This study included performing a theoretical analysis of the reactor characteristics, evaluating the technological problem areas, defining a conceptual design of a ground test reactor (GTR) and recommending a test program for the reactor development. The reactor characteristics are given in Table 1.

Figure 1 shows the schematic diagram of the cavity reactor configuration and hydrogen flow paths. This paper describes

the conceptual design of a ground test reactor for this concept. Some technological problem areas are also suggested.

## Fuel Selection

### Fuel Composition

The use of alloy fuel particulates was based on a thermodynamic consideration. Because of the highly effective separation of fuel and propellant that can be achieved by a vortex chamber, the only loss of fuel considered was the uranium vapor carried out by the propellant.<sup>¶</sup> To minimize the vapor loss the fuel should have a low uranium equilibrium vapor pressure. The vapor pressure data of the ternary system involving U-C-Zr are based on the thermodynamic formulation of free energy as suggested by Kaufman and Peters,<sup>6</sup> expressed in terms of partial and vapor pressures of each element. The vapor composition in equilibrium with the solid fuel can then be computed at a given pressure and temperature. This yields the molecular weight of the vapor mixture  $M_t = \sum_i M_i P_i / P_t$  from which the specific impulse of the rocket exhaust and the uranium loss rate can be evaluated for a given thrust engine.  $I_{sp} = (M_H / M_t)^{1/2} (I_{sp})_H$ , where the specific impulse  $(I_{sp})_H$  and molecular weight for hydrogen,  $M_H$ , are obtained as a function of  $P_s$  and  $T_s$  from real gas nozzle calculations at a fixed pressure ratio.<sup>7</sup> Figure 2 shows the performance vs pressure-temperature conditions. The solid lines represent loci of constant specific impulse and

**Table 1 Characteristics and dimensions of the colloid-core ground test reactor**

|   |                         |
|---|-------------------------|
| Thrust capability                                     | 100,000 lbf (45,000 kg) |
| Specific impulse (theoretical)                        | 1200 sec                |
| Static pressure at the inlet of exhaust nozzle        | 100-200 atm             |
| Static temperature at the inlet of the exhaust nozzle | 3700°K-3900°K           |
| Fuel Zr and U carbide alloy                           | (1U-10Zr)C              |
| Cavity diameter                                       | 120 cm (47.5 in.)       |
| Cavity fuel suspension zone length                    | 18 cm (7 in.)           |
| Radial reflector thickness                            | 45 cm (17.7 in.)        |
| Axial length of reflector                             | 108 cm (42.5 in.)       |
| Reflector annulus fueled zone thickness               | 15 cm (5.9 in.)         |
| Pressure vessel outer diameter                        | 240 cm (95 in.)         |
| Over-all length                                       | 240 cm (95 in.)         |
| Total engine weight (less storage)                    | 41,000 lb (19,000 kg)   |

<sup>¶</sup> Although the loss of fine particles has been neglected in the fuel loss analysis, it has been shown in Ref. 5 that particle losses due to imperfect containment of the order of only a few percent were obtainable. This is certainly within the accuracy of calculation for the vapor loss to be shown.

Presented as Paper 70-688 at the AIAA 6th Propulsion Joint Specialist Conference, San Diego, Calif., June 15-19, 1970; submitted July 1, 1970; revision received October 13, 1970. This work was conducted under contract from the Aerospace Research Laboratory of Wright-Patterson Air Force Base, Ohio.

\* Advisory Engineer, Systems & Technology Department, Westinghouse Astronuclear Lab.

† Senior Engineer, Power and Propulsion, Systems & Technology Department, Westinghouse Astronuclear Lab.

‡ Manager of Advanced Projects, Systems & Technology Department, Westinghouse Astronuclear Lab.

§ Manager of Physics and Mathematics, NERVA Project, Westinghouse Astronuclear Lab.

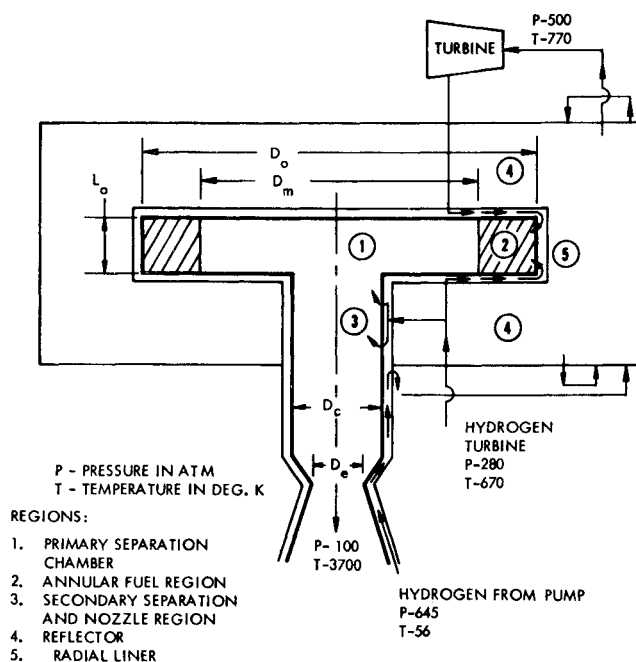


Fig. 1 Schematic of cavity reactor configuration.

the dotted lines represent constant uranium loss rates. These uranium loss rates are based on calculated vapor pressures that require experimental verification. It should also be noted that actual values of specific impulse are lower than the ideal values shown in this figure, which can be obtained by a nozzle discharge coefficient to take into account the heat and frictional losses. Within the range of specified pressure and temperature, the uranium loss rate is 28–30 kg/min, corresponding to a uranium to hydrogen flow rate of  $\frac{1}{80}$ .

#### U-233 vs U-235 Fuel

The advantage of U-233 fuel as opposed to U-235 fuel can be determined by examining the microscopic cross-section data of both uranium isotopes. The average number of neutrons per fission of U-233 is slightly higher than that produced per fission of U-235 over the entire neutron energy spectrum range, which provides a very slight advantage to

U-233. The primary advantage of U-233 is in its higher neutron efficiency, or its lower capture to fission cross-section ratio  $\alpha$ , relative to that of U-235. In addition, this ratio for U-235 increases rapidly as the intermediate spectrum is approached, while the  $\alpha$  of U-233 remains relatively constant. This particular characteristic of the two isotopes takes on added significance if neutronically poisonous liner materials must be used, as in the present design. The return neutron current at the cavity-liner interface is sharply shifted from the thermal to the epithermal and fast energy groups. U-233, with a relatively constant  $\alpha$ , is less affected by this spectral shift than U-235. For comparison purposes, a spherical reactor was used with a cavity radius of 50 cm, and reflector outer radii of 85 and 95 cm. The required cavity fuel loading is shown in Fig. 3 as a function of the optical thickness of the liner material for both isotopes.

#### Particle Size and Fission Fragmentation

The slowing down of fission fragments in fuel material can cause ejection of fuel material from the fuel body. The fuel loss would be proportional to the number of fission fragments escaping from the fuel, and the latter decreases with increasing particle size. Assuming the ejected fuel material is in the form of clumps containing  $10^4$  atoms of uranium<sup>8</sup> on the average, and every tenth fission fragment causes fuel ejection, it was estimated for fuel particles of  $100\mu$  in diameter, at a flux of  $10^{13} \text{ cm}^{-2}, \text{ sec}^{-1}$  that the loss rate may be 10% of core loading per minute. On the other hand, if the fuel particles are sufficiently reduced, it is conceivable that the fission fragments may escape from the fuel particle before enough energy to displace  $10^4$  atoms has been transferred to the fuel. Using this criterion, and assuming two fission fragments results from each fission and the mass and charges estimated by Brinkman,<sup>9</sup> a particle diameter  $\leq 0.1\mu$  for (1U-10Zr)C would be required. However, such a small diameter would be impractical from the manufacturing and quality control viewpoints. Pending further development in the effects of the agglomeration and the fragmentation phenomena, a preliminary selection of the particle size in the range of  $0.5\text{--}5\mu$  was made for the ground test reactor. This was based on the consideration that particle sizes larger than this range may impinge on the cavity liner.

#### Vortex Chamber

The vortex chamber, or cavity, configuration evolved from the hydrodynamic experiments that were conducted by ARL.<sup>11</sup> Figure 1 illustrates the chamber geometry thus defined and identifies major regions. The cavity region 2, having a length to diameter ratio ( $L_0/D_0$ ) much less than unity, characterizes this geometry as a compressed cavity. It has been shown to provide an increased capability for the retention of relatively large masses of solid particles. The primary function of the vortex chamber is to separate and retain fuel particles in the chamber with the solid-free gas exhaust at the exit end ( $D_e$ ). By nature of the vortex flow, the portion serves the function of a final clean-out stage of the exhaust gas. The finest particles in the exhaust gas stream may thus be centrifuged to the wall in region 3, where they will be carried to the closed end of the chamber. The second consideration of the cavity configuration is the tendency of particles to impinge on the peripheral wall. Because the centrifugal force acting on the particles varies with  $(v^2/r)$ , increasing the radius  $r$ , with the accompanying effect of a reduction in the tangential velocity  $v$ , will reduce the centrifugal force rapidly. Consequently, the tendency of particle impingement on the wall can be reduced by means of a large diameter  $D_0$ . To aid in the selection of the dimensions  $D_0$  and  $L_0$ , a nuclear parametric study was made over a wide range of reactor sizes having the basic configuration. The variable  $D_0$  was allowed to vary from 60 to 180 cm while

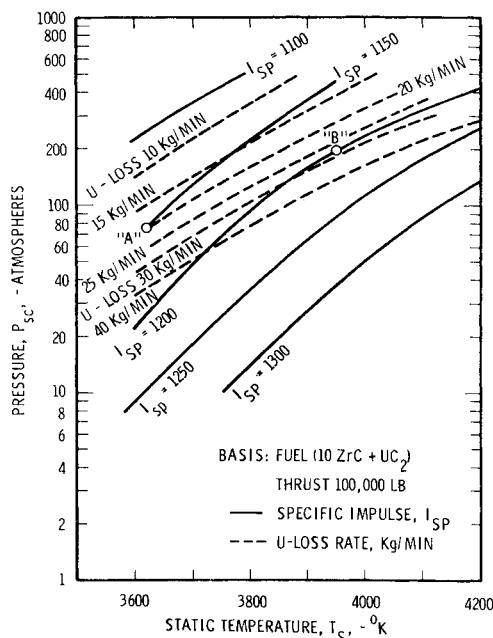


Fig. 2 Performance vs pressure-temperature conditions.

the  $(L_0/D_0)$  ranged from 0.10 to 0.20. Referring to Fig. 1, a uniform distribution of fuels was assumed over region 2, and a 4-mil natural tungsten liner was placed in region 5. The axial and radial reflectors, regions 4 and 5, are assumed 45 cm thick and made of beryllium. Of principal interest were the critical mass requirement and the resulting solid loading factors in the cavity fuel region 2. The two-dimensional discrete ordinates transport theory code (DOT)<sup>11</sup> was used in the nuclear calculations. Figure 4 presents the results of these calculations where critical masses are plotted vs the outer fuel diameter  $D_0$  with three cavity length-to-diameter ratios. Based on this, and the hydrodynamic considerations mentioned previously, a configuration with  $D_0 = 120$  cm and  $L_0/D_0 = 0.15$  was chosen.

### Propellant Cycle and Fueled Reflector

Both bleed and topping cycles were considered for propellant pumping power. The bleed cycle was found undesirable because of the high percentage bleed flow required at a discharge pressure of 8000–9000 psi. Due to the low pressure available in a bleed cycle, a large number of bleed turbine stages would be needed. The reactor design, therefore, uses a topping cycle. From thermal calculations of the propellant cycle including the fraction of fission energy deposited in the reflector and the thermal power requirement of the turbopump system, it became obvious that additional heating in the reflector is required. The amount of energy deposited in the reflector was evaluated by considering the energy generated by prompt gamma rays, the prompt gamma ray energy release from neutron radiative capture and inelastic scattering, and neutron kinetic energy from nuclear fission.<sup>12</sup> For a 2000 Mw reactor this amounts to 200 Mw, but the thermal power required to the inlet of turbopump system is in the range of 320–400 Mw. The additional heating can be realized by fueling a portion of the reflector.

The effect on the specific impulse of preheating the propellant before it enters the cavity reactor can be shown by the definition of specific impulse, which is proportional to the square root of the temperature of the exhaust gases just before they enter the nozzle throat divided by the average molecular weight of the gases. Using enthalpy instead of temperatures, it becomes

$$I_{sp} = \text{const}(h)^{1/2} \quad (1)$$

Assuming that the enthalpy per unit mass of hydrogen in the storage is  $h_0 = 0$ , and that the hydrogen is preheated to  $h_s$  by solid-fueled region in the reflector at temperature  $T_s$ , the final enthalpy of the hydrogen at the exit of the colloid-fueled reactor will be  $h_c$  at temperature  $T_c$ . Expressed in terms of the fraction of the total fission energy produced in the solid-fueled region  $f$ , the enthalpy ratio becomes

$$h_c = h_s/[f + \beta(1 - f)] \quad (2)$$

where  $\beta$  is the fraction of fission energy from the cavity which is deposited in the reflector and the exhaust nozzle, etc. Consequently, the specific impulse at the exit nozzle  $I_c$  can be obtained from the following:

$$I_c^2 = I_s^2/[(1 - \beta)f + \beta] \quad (3)$$

where  $I_s$  is the specific impulse corresponding to  $h_s$  at the exit of the solid-fueled region. Since the value of  $I_s$  is limited by the material in the solid-fueled region, the maximum  $I_c$  can be approached by minimizing the fraction  $f$ .

If the maximum hydrogen temperature out of the fueled reflector  $T_s$  is 870°K, the ratio of  $(I_c/I_s)$  becomes  $(1200/580)$ . Assuming the value of  $\beta = 0.11$ , the fraction of fission produced in the reflector should be, for the topping cycle,  $f = 0.13$ . In addition to the power required for the turbopump under normal operating conditions, the preheating of propellant during start-up is more important because the vortex

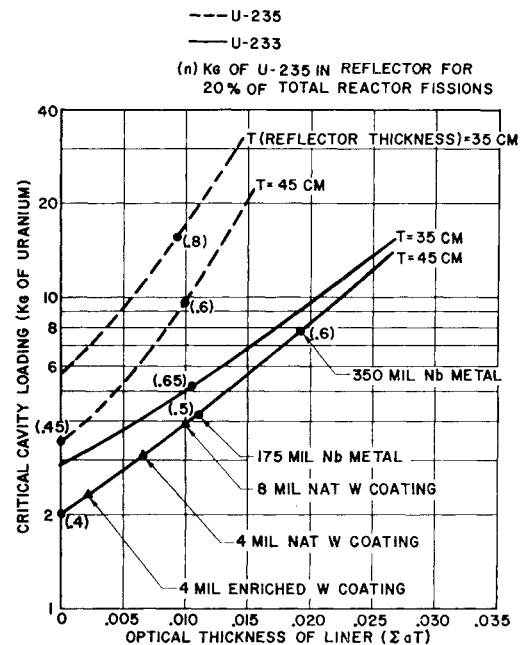


Fig. 3 Cavity critical mass vs optical thickness of liner.

set up by the propellant must be established before a critical mass can be retained in the cavity. A critical reflector with reflector-located control drum concept suggests a realistic approach-to-criticality. Sufficient fuel is placed in the reflector to make the reactor critical with no fuel in the cavity. Control drums located in the reflector would be rotated until the reactor becomes critical with the reflector fuel only. Hydrogen would be initially introduced into the system using tank pressure. The reflector would be brought to power by rotating the drums, generating power commensurate with the amount of hydrogen entering the system. The heated hydrogen would drive the turbopump, increasing the hydrogen flow. The reflector power would be increased simultaneously until, in this boot-strap manner, sufficient energy is being generated such that the hydrogen introduced into the cavity would be up to full pressure and flow conditions. Next, fuel would be introduced into the cavity. As the fuel is being added, thus increasing reactivity and power in the cavity region, the reflector control drums would be rotated to reduce the reactivity of the reflector and keep the power in the reflector at the level necessary to maintain the vortex. Eventually, when the desired power level is achieved in the cavity region, the drums would be in such a position that 13% of the total thermal power would be generated in the reflector

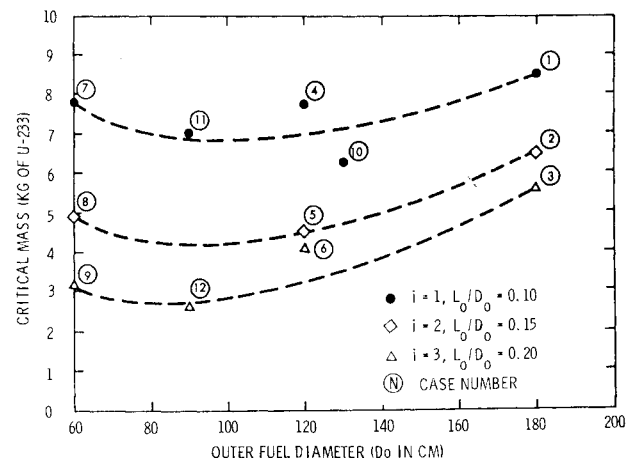


Fig. 4 Critical mass vs o.d. ( $D_0$ ).

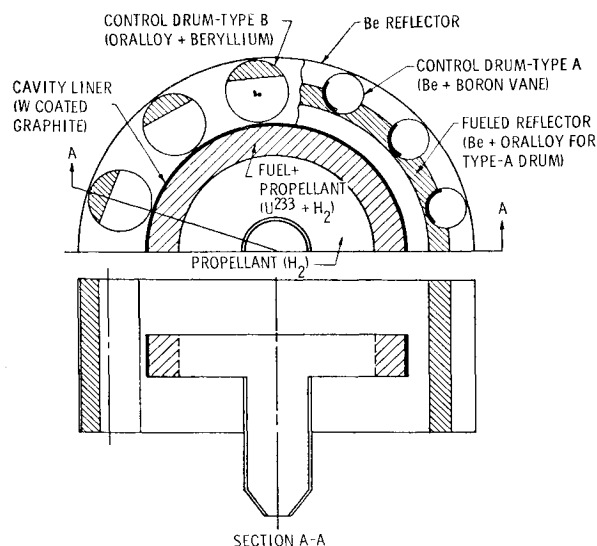


Fig. 5 Schematic of low  $L/D$  cylindrical cavity reactor with mechanical control system.

due to fission.\*\* The additional power would then come from radiative heating due to energy deposition from the cavity. Two possible control drum arrangements were investigated for the GTR which are described in the next section.

### Control of Reactivity in the Reflector

Figure 5 illustrates a possible arrangement of control drums in the reflector for two types (A and B) of control concepts. The type A concept uses poison vanes (composed of boron-10 in stainless steel, for example) placed around fixed (sleeve concept) or rotating (attached vane) beryllium drums. As the poison vanes are rotated outward from the center of the fueled annulus in the reflector (minimum reactivity position), reactivity would increase. At some point near the full-out position, the reactor would be critical with no fuel in the cavity. The type B control drums, also shown in Fig. 5, are partially fueled beryllium drums. Initially, the fueled portion of the drums would be in the full-out (minimum reactivity) position. As the fueled portion of the drums rotates inward to a higher importance region within the reflector, reactivity would increase. Sufficient fuel would be placed in the drums to make the reactor critical at some position near full-in without fuel in the cavity.

The type A, rotating position vane, concept was chosen for the GTR because: 1) the rotating vane configuration allows a considerably larger fueled reflector volume than can be provided for with rotating fuel segments. This results in a lower fission density or heating rate in the rotating vane concept and thus poses a less stringent cooling requirement in the reflector; and 2) the inertia of the fuel segments in a rotating fueled drum would have required considerably more massive control drives to achieve a given rate of reactivity insertion relative to the rotating vane design.

### Reactor Conceptual Design

The components of the GTR design are shown in Fig. 6. This reactor consists of three major parts: the outer pressure enclosure, the inner pressure enclosure, and the nozzle. The outer enclosure consists of a cylindrical pressure vessel (titanium alloy Ti-Al-V) with dome-end and nozzle-end

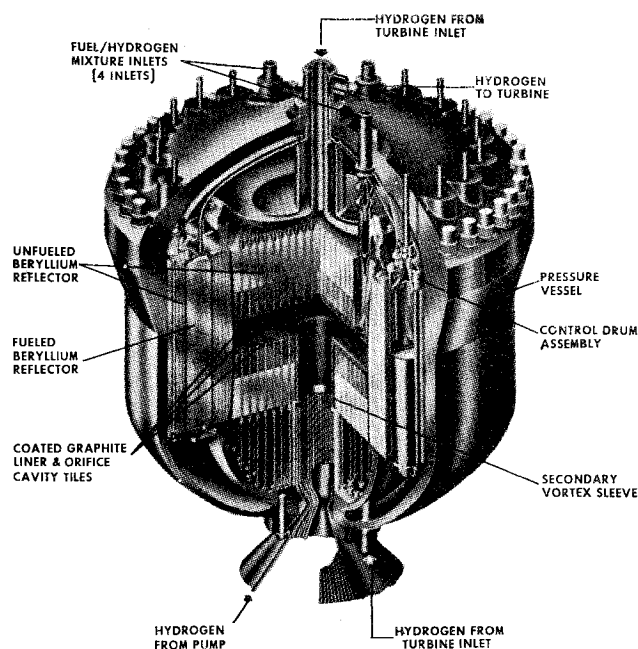


Fig. 6 Principal components colloid core reactor.

sections, unfueled radial beryllium reflector, fueled radial beryllium reflector, and control drums. The inner enclosure consists of a cylindrical pressure vessel with dome-end and nozzle-end sections, dome-end axial reflector and nozzle-end axial reflector and inconel support tubes and cavity liners. The nozzle consists of nozzle sections, graphite nozzle vortex sleeve, and the flange. The significant dimensions of the cavity and reflector and the reactor characteristics are shown in Table 1.

The cooling of the reactor components is obtained by passing the propellant gas through them. The cold hydrogen gas enters the nozzle skirt, flows around the inside perimeter of the pressure vessel, and exits to the turbine inlet after passing through the fueled radial reflector sectors and control drums. From the turbine the flow re-enters through the dome-end and nozzle-end reflector assemblies, around the cavity-liner tiles, into the cavity through the cavity orifice tiles, and then out the nozzle exit. There are 1700 orifices of 0.38 cm diam that inject the gas with a tangential velocity of about 110 m/sec.

The temperature limit of the reflector material and the erosive nature of colloid fuel necessitates the use of a cavity liner. The selection of material and the design of the liner must meet the requirements from the nuclear and thermal environment as well as the structural requirement. The final solution lies in the combination of several features. The reflector material, beryllium, when kept below 810°K, is able to bear a pressure load. The graphite, as a liner, can withstand high temperatures and will not be subjected to thermal stresses when used in the form of small tiles. For further protection from the hot hydrogen and erosive particulate material, the graphite is coated by deposited tungsten.

The design of the pressure vessel depends on the shape of the cavity and reflector. Provisions for cooling the vessel are desirable to keep the material in the temperature range of maximum strength. The use of special material such as glass filament-wound vessels requires considerable development<sup>13</sup> in the area of joint design, porosity to high pressure hydrogen, and radiation effects on glass filaments under stresses. Because the pressure vessel accounts for more than 60% of the total weight, optimizing the shape or design of the reflector and vessel will have significant effect on the weight. For the GTR reported in this paper, no attempt was made to optimize the weight of the system.

\*\* In the GTR the reflector fission fraction is larger than 0.13. Thus, in order to maintain the exhaust temperature at the fixed value, the propellant flow through the exhaust nozzle is reduced.

### Conclusions

From the results of this study, the following conclusions emerge:

1) The colloid core concept is feasible from the standpoint of reactor design. With a solid particulate fuel a specific impulse of 1200 lb-sec/lb<sub>m</sub> is obtainable.

2) The preliminary design of the GTR resulted in a weight of about 41,000 lb (or 19,000 kg) for a thrust of 100,000 lb (45,000 kg). No attempt was made to optimize the weight of the ground test system.

3) Several technological problem areas requiring further examination may be recommended, i.e.: a) fuel vaporization losses, b) fuel particle fission fragmentation, and c) liner material erosion.

### References

- <sup>1</sup> Gabriel, D. S. and Helms, I. L., "Nuclear Rocket Engine Program Status-1970," AIAA Paper 70-711, San Diego, Calif., 1970.
- <sup>2</sup> Rom, F. E., "Comments on the Feasibility of Developing Gas Core Nuclear Reactors," TMX-52644, 1969, NASA.
- <sup>3</sup> McLafferty, G. H., "Gas Core Nuclear Rocket Engine Technology Status," AIAA Paper 70-708, San Diego, Calif., 1970.
- <sup>4</sup> Tang, Y. S., Stefanko, J. S., and Dickson, P. W., "The Colloid Core Concept A Possible Forerunner for the Gaseous

Core," *Symposium on Uranium Plasmas*, Univ. of Florida, Gainesville, Fla., 1970.

<sup>5</sup> Pinchak, A. C. and R. Poplawski, "On the Attainment of Extremely High Rotational Velocities in a Confined Vortex Flow," AIAA Paper 65-400, San Francisco, Calif., 1965.

<sup>6</sup> Kaufman, L. and E. T. Peters, "Analysis of Vaporization in Liquid Bearing Systems of Very High Temperatures," CR-353, 1965, NASA.

<sup>7</sup> King, C. R., "Compilation of Thermodynamic Properties and Theoretical Rocket Performance of Gaseous Hydrogen," TN D-275, 1960, NASA.

<sup>8</sup> Rogers, M. D., "Mass Transfer and Grain Growth Induced by Fission Fragments in Thin Films of Uranium Dioxide," *Journal of Nuclear Materials*, Vol. 16, No. 3, 1965, p. 298.

<sup>9</sup> Brinkman, J. A., "Fission Damage in Metals," NAA SR-6642, March 1962, NASA.

<sup>10</sup> Jackomis, W. N. and Von Ohain, H. J. P., "Aeromechanical Characteristics of Nuclear Reactor Cavities Using Colloidal Fuels," AIAA Paper 70-1222, Houston, Texas, 1970.

<sup>11</sup> Mynatt, F. R., "A User's Manual for DOT Program—A Two-Dimensional Discrete Ordinate Transport Code with Anisotropic Scattering," Rept. K-1694, 1967, ORNL.

<sup>12</sup> Westinghouse Astronuclear Laboratory, "Engineering Study of Colloid Fueled Nuclear Rocket," Rept. 69-0234, Dec. 1969, Aerospace Research Labs.

<sup>13</sup> Sieder, F. G. and Martin, G. H., "Filament-Wound Pressure Vessel Design Study for Nuclear Light Bulb Engine," Rept. F-910093-37, Appendix A, 1967, United Technology Center, United Aircraft Corp.

## Parametric Investigation of Mercury Hollow-Cathode Neutralizers

D. C. BYERS\* AND AARON SNYDER†  
NASA Lewis Research Center, Cleveland, Ohio

A parametric investigation of mercury hollow-cathode neutralizers for Kaufman ion thrusters was carried out in a bell jar over a range of collector (ion beam simulator) currents up to 2 amp. The parameters investigated included mercury neutral flow rate, neutralizer cathode geometry, collector geometry and spacing, keeper power supply impedance, keeper current, keeper electrode geometry and spacing. Agreement was found between neutralizer operation in the bell jar and on an active thruster. The influence of the various parameters on neutralizer performance and control characteristics is discussed for three distinct modes of neutralizer operation.

### Introduction

HOLLOW-CATHODE neutralizers<sup>1</sup> appear to be suitable for use with thrusters which operate over a large range of ion beam currents.<sup>2-4</sup> Such neutralizers have been studied for a variety of specific thruster operating conditions.<sup>5-8</sup> Neutralizer optimization programs have been carried out or are in progress with 5-, 15-, and 30-cm-diam thrusters.<sup>2-4</sup> It was found in these programs that the optimum neutralizer design was specific to the emission currents (equal to ion beam currents) and neutral flow rates at which the neutralizer was required to operate. Studies have been made of the effects of various neutralizer parameters,<sup>6,9</sup> but most investigations have been concerned with a limited range of

neutralizer operating conditions and/or a specific neutralizer configuration.

Neutralizer performance is defined in terms of the required neutral flow rates, operating voltages, and power levels. The neutral flow rate is charged directly against the over-all thruster system propellant utilization efficiency, the operating voltages are directly related to neutralizer lifetime, thrust, and over-all thruster system power efficiency. The neutralizer system must also be amenable to some type of control logic. Some parameters, such as coupling voltage, must generally be held or controlled within certain limits to avoid degradation of performance or lifetime.<sup>5</sup> On the SERT II thruster, for example, the keeper voltage (which is proportional to coupling voltage) is sensed and controlled via a feedback loop with the neutralizer vaporizer.<sup>2</sup> The relationship between the controlled and control parameters must be known and of such a form as to allow a stable control loop logic.

This paper presents the results of a bell-jar investigation of various hollow-cathode neutralizers over a wide range of operating parameters. A comparison also was made between

Presented as Paper 70-1090 at the AIAA 8th Electric Propulsion Conference, Stanford, Calif., August 31-September 2, 1970; submitted September 18, 1970; revision received December 2, 1970.

\* Aerospace Research Engineer. Member AIAA.

† Student Trainee.